Journal of Structural Biology xxx (2017) xxx–xxx

Contents lists available at ScienceDirect

Journal of Structural Biology

journal homepage: www.elsevier.com/locate/yjsbi

Tracking the amyloidogenic core of IAPP amyloid fibrils: Insights from micro-Raman spectroscopy

Nikolaos N. Louros [a,1], Paraskevi L. Tsiolaki [a], Fotis A. Baltoumas [a], Georgios D. Chryssikos [b], Vassilis Gionis [b], Stavros J. Hamodrakas [a], Vassiliki A. Iconomidou [a,*]

[a] Section of Cell Biology and Biophysics, Department of Biology, School of Sciences, National and Kapodistrian University of Athens, Panepistimiopolis, Athens 157 01, Greece
[b] Theoretical and Physical Chemistry Institute, National Hellenic Research Foundation, Athens 116 35, Greece

ARTICLE INFO

Article history:
Received 22 February 2017
Received in revised form 19 May 2017
Accepted 3 June 2017
Available online xxxx

Keywords:
Amylin
Amyloidosis
Aggregation-prone peptides
Disulfide bonds
Type II diabetes
Raman Spectroscopy

ABSTRACT

Human islet amyloid polypeptide (hIAPP) is the major protein component of extracellular amyloid deposits, located in the islets of Langerhans, a hallmark of type II diabetes. The underlying mechanisms of IAPP aggregation have not yet been clearly defined, although the highly amyloidogenic sequence of the protein has been extensively studied. Several segments have been highlighted as aggregation-prone regions (APRs), with much attention focused on the central 8–17 and 20–29 stretches. In this work, we employ micro-Raman spectroscopy to identify specific regions that are contributing to or are excluded from the amyloidogenic core of IAPP amyloid fibrils. Our results demonstrate that both the N-terminal region containing a conserved disulfide bond between Cys residues at positions 2 and 7, and the C-terminal region containing the only Tyr residue are excluded from the amyloid core. Finally, by performing detailed aggregation assays and molecular dynamics simulations on a number of IAPP variants, we demonstrate that point mutations within the central APRs contribute to the reduction of the overall amyloidogenic potential of the protein but do not completely abolish the formation of IAPP amyloid fibrils.

1. Introduction

Islet amyloid polypeptide (IAPP), or amylin, is a 37-residue pancreatic hormone produced and secreted along with insulin as a response to high levels of glucose within the bloodstream. IAPP is a highly amyloidogenic peptide, primarily associated with the development of type II diabetes (Clark et al., 1987; Cooper et al., 1987). IAPP accumulation within the islets of Langerhans eventually causes β-cell dysfunction and death, consequently leading to reduced insulin secretion (Westermark and Wilander, 1978; Westermark et al., 1987a). The toxic effect of hIAPP is a subject of controversy, in which amyloid-mediated membrane damage is considered to play a key role. A two-fold mechanism of aggregation has been proposed, suggesting that initial membrane disruption is caused by early oligomeric IAPP species that can also template amyloid fiber formation on the membrane surface at a later stage, a process leading to subsequent fragmentation (Brender et al., 2012; Patel et al., 2014; Sciacca et al., 2016). The N-terminal 1–19 region of the peptide is primarily responsible for membrane binding by controlling the orientation and penetration depth of the molecule in respect to the membrane surface (Nanga et al., 2009). On the other hand, almost the entire sequence of human IAPP has been denoted as an aggregation-prone region (APR), suggesting that the aggregation effect of the protein may not be as straightforward as expected (Azriel and Gazit, 2001; Fox et al., 2010; Lutz, 2010; Marek et al., 2007). Several lines of evidence have focused at the aggregation potential of the 20–29 central segment. Comparison studies reveal significant differences in the structure, function and toxicity kinetics between the corresponding regions of human and rat IAPP sequences ($hIAPP_{20-29}$ and $rIAPP_{20-29}$) (Brender et al., 2007, 2013). This is mostly attributed to the fact that the non-amyloidogenic $rIAPP_{20-29}$ sequence comprises three individual Pro residues within this range, imparting its overall aggregation tendency (Christoffersen et al., 2015; Madine et al., 2008; Moriarty and Raleigh, 1999; Westermark

Abbreviations: hIAPP, human IAPP; rIAPP, rat IAPP; APRs, aggregation-prone regions; STEM, scanning-transmission electron microscopy; ssNMR, solid-state Nuclear Magnetic Resonance; RMSF, root mean square fluctuation; ASA, accessible surface area; TERS, Tip-Enhanced Raman Spectroscopy.

* Corresponding author.
E-mail addresses: nlouros@biol.uoa.gr (N.N. Louros), etsiolaki@biol.uoa.gr (P.L. Tsiolaki), fbaltoumas@biol.uoa.gr (F.A. Baltoumas), gdchryss@eie.gr (G.D. Chryssikos), vgionis@eie.gr (V. Gionis), shamodr@biol.uoa.gr (S.J. Hamodrakas), veconom@biol.uoa.gr (V.A. Iconomidou).
[1] Present address: VIB Switch Laboratory, Department of Cellular and Molecular Medicine, VIB-KU Leuven, B-3000 Leuven, Belgium.

http://dx.doi.org/10.1016/j.jsb.2017.06.002
1047-8477/

et al., 1990). An amylin replacement has been developed based on this strategy and is currently administered along with insulin in patients with type I and II diabetes (Ratner et al., 2004).

Although accumulating evidence suggests that IAPP is intrinsically disordered or partially α-helical in its active and functional form (Nanga et al., 2011; Williamson and Miranker, 2007), the structural properties of IAPP monomers incorporated in amyloid fibrils are yet poorly understood. Detailed NMR structural studies on human and rat peptides have highlighted that the 1–19 region of the molecule is primarily α-helical, suggesting that helical intermediates promote the overall toxicity of IAPP by facilitating membrane disruption (Brender et al., 2010; Nanga et al., 2009). Up to date, a number of theoretical or experimental studies have proposed possible models regarding the fibrillar core of human IAPP amyloid fibrils. A parallel superpleated structure, composed of three individual β-strands was initially proposed (Kajava et al., 2005), followed by ssNMR and STEM observations suggesting that the 8–17 and 28–37 segments of the protein compose the main fibril core (Luca et al., 2007). This model was also supported subsequently by two-dimensional infrared spectroscopy (IR) studies (Shim et al., 2009). Finally, a third model has also been proposed, relying on the atomic structures of segments 21–27 and 28–33 which were suggested to form tight steric zippers with closely interdigitated side chains (Wiltzius et al., 2008).

In this work, we applied micro-Raman spectroscopy on aligned IAPP amyloid fibrils to extract information about the structural elements that are part of the amyloidogenic core, in addition to the conformational states and orientation of individual moieties, such as the N-terminally located intermolecular disulfide bridge, the β-sheet content and the C-terminal Tyr side chains of the IAPP monomers. Furthermore, we performed detailed aggregation assays on several variants focused around the major 8–17 and 20–29 APRs of the IAPP sequence. These results are complemented with Molecular Dynamics (MD) simulations and discussed in comparison with the existing reported models regarding IAPP amyloid fibrils.

2. Materials and methods

2.1. Aggregation propensity prediction

The aggregation propensity of human IAPP was investigated through sequence analysis, with the aid of the consensus aggregation propensity predictor, AMYLPRED2 (Tsolis et al., 2013). This consensus tool produces a multivariate prediction of sequence amyloidogenicity by incorporating individual algorithms, focused on identifying variable physicochemical properties associated with aggregation propensity, such as sequence hydrophobicity, packing density, "chameleon" segments and amyloidogenic sequence stretches (Conchillo-Sole et al., 2007; Fernandez-Escamilla et al., 2004; Kim et al., 2009; Tian et al., 2009).

2.2. Peptide synthesis

The synthesis of human wild type (WT) IAPP and its mutated derivatives (Fig. 1) was performed by GeneCust (Luxembourg). All peptides were prepared with amidated C-terminal ends and free N-terminals (purity >95%). $IAPP_{1-12}$ (free N- and C-terminal) was prepared by solid phase methodology and Fmoc/Bu^t chemistry, using 2-chlorotrityl chloride resin as a solid support (Barlos et al., 1989). Analytical HPLC was utilized in order to determine peptide purity (>97%).

2.3. Preparation of peptide samples and oriented fibers

Solution samples of IAPP and its derivatives were prepared at a concentration of 0.5 mg/ml, in distilled water. The $IAPP_{1-12}$ peptide

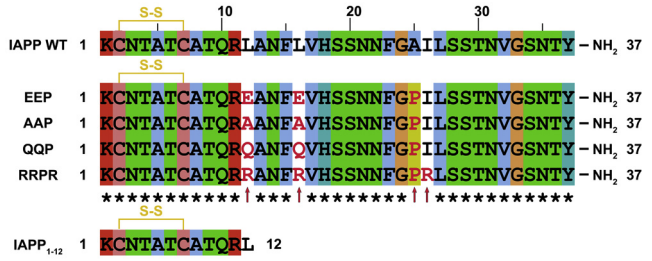

Fig. 1. Sequence of human IAPP and its mutated derivatives. Four different variants were designed by replacing residues L12 and L16 to charged, polar or other hydrophobic residues (EEP, RRPR, QQP and AAP peptides). All peptides have a single substitution of A25P, whereas the RRPR peptide also incorporates an additional I26R mutation. All variants were C-terminal amidated and contained an intramolecular disulfide bond (shown in yellow brackets). A peptide analogue of the N-terminal segment of IAPP was also designed ($IAPP_{1-12}$).

segment was dissolved at peptide concentrations up to 10 mg/ml. Oriented fibers containing more or less aligned amyloid fibrils were prepared after 1–2 weeks of incubation at ambient temperature, by applying a droplet (5 μl) of each peptide solution between aligned glass rods with silicone-covered ends, spaced approximately 2 mm apart. The droplets were slowly air-dried at ambient conditions to produce oriented fibers suitable for X-ray diffraction and micro-Raman spectroscopic analysis. $IAPP_{1-12}$ solutions were incubated for long periods of up to six months, however were incapable of forming well-oriented fibers. As a result, suspensions of this peptide were cast on a front-coated Au mirror and left to dry in ambient conditions to form films suitable for micro-Raman measurements.

2.4. Transmission electron microscopy

Suspensions of each peptide were placed on carbon-coated copper grids and allowed to sit for 60 s. Subsequently, the grids were flash-washed with distilled water and stained with a drop of 2% (w/v) aqueous uranyl acetate for 45 s. Excess stain was removed by blotting with a filter paper. A Morgagni™ 268 transmission electron microscope, operated at 80 kV, was used for examination of prepared grids. Digital micrographs were acquired with an 11 Mpixel, side-mounted Morada CCD camera (Soft Imaging System, Muenster, Germany).

2.5. X-ray diffraction

X-ray diffraction patterns were collected from oriented fibers, using a SuperNova-Agilent Technologies X-ray generator, operated at 50 kV and 0.8 mA, equipped with a 135-mm ATLAS CCD detector and a 4-circle kappa goniometer (CuK_α high intensity X-ray microfocus source, $\lambda = 1.5418$ Å). Specimen-to-film distance was specified at 52 mm, whereas exposure time was set to 400 s. Initial viewing was performed using the program CrysAlisPro (Oxford Diffraction, 2009). The X-ray diffraction patterns were measured and displayed with the aid of iMosFLM (Leslie and Powell, 2007).

2.6. Congo red staining assays

Drops of all peptide solutions were applied to glass slides and air-dried at ambient conditions, producing hydrated films. A Congo red solution (1% w/v) was prepared in distilled water and used to stain the hydrated films, following previous protocols (Louros et al., 2014, 2015a; Romhanyi, 1971). Excess stain was removed by rinsing in water (Romhanyi, 1971). Stained samples were observed under bright field illumination and between crossed polars, utilizing a Leica MZ7.5 polarizing stereomicroscope

Please cite this article in press as: Louros, N.N., et al. Tracking the amyloidogenic core of IAPP amyloid fibrils: Insights from micro-Raman spectroscopy. J. Struct. Biol. (2017), http://dx.doi.org/10.1016/j.jsb.2017.06.002